

10. Frank-Raue K, Raue F, Buhr HJ, Baldauf G, Lorenz D, Ziegler R. Localization of occult persisting medullary thyroid carcinoma before microsurgical reoperation: high sensitivity of selective venous catheterization. *Thyroid* 1988;2:113-117.
11. Perkins A. Perioperative nuclear medicine. *Eur J Nucl Med* 1993;20:573-575.
12. Fraker DL, Norton JA. The role of surgery in the management of islet cell tumors. *Gastroenterol Clin North Am* 1989;18:805-830.
13. Arnold MW, Schneebaum S, Berens A, et al. Intraoperative detection of colorectal cancer with radioimmunoguided surgery and CC 49, a second-generation monoclonal antibody. *Ann Surg* 1992;216:627-632.
14. Moffat FL, Vargas-Cuba RD, Serafini AN, et al. Preoperative scintigraphy and operative probe scintimetry of colorectal carcinoma using technetium-99m-88BV59. *J Nucl Med* 1995;36:738-745.
15. Schirmer WJ, O'Dorisio TM, Schirmer TP, Mojzisk CM, Hinkle GH, Martin EW. Intraoperative localization of neuroendocrine tumors with ¹²⁵I-TYR (3)-octreotide and a hand-held gamma-detecting probe. *Surgery* 1993;114:745-752.
16. Adams S, Baum RP, Wenisch HJC. Intraoperative localization of recurrent medullary thyroid carcinoma with a hand-held gamma probe. In: Reinwein D, Weinheimer B, eds. *Therapy of hyperthyreosis*, 11th ed. Berlin: de Gruyter; 1994:508-512.
17. Frucht H, Doppmann JL, Norton JA, et al. Gastrinomas: comparison of MR imaging with CT, angiography, and US. *J Clin Endocrinol Metab* 1990;71:566-574.
18. Günther RW, Klose KJ, Rückert K. Islet tumors: detection of small lesions with CT and ultrasound. *Radiology* 1983;148:485-488.
19. Hemmingson A, Lindgren PG, Lörelus LE, Öberg K. Diagnosis of endocrine gastrointestinal tumors. *Acta Radiol* 1981;22:657-662.
20. Scherübl H, Faiss S, Zimmer T, Riecken EO, Wiedenmann B. Neuroendocrine tumors of the gastroenteropancreatic system. I. *Diagn Adv Oncol* 1996;19:119-124.
21. Kwekkeboom DJ, Krenning EP, Bakker WH, et al. Somatostatin analog scintigraphy in carcinoid tumors. *Eur J Nucl Med* 1993;20:283-292.
22. Kwekkeboom DJ, Lamberts SWJ, Habbema JDF, Krenning EP. Cost-effectiveness analysis of somatostatin receptor scintigraphy. *J Nucl Med* 1996;37:886-892.
23. Schillaci O, Scopinaro F, Angeletti S, et al. SPECT improves accuracy of somatostatin receptor scintigraphy in abdominal carcinoid tumors. *J Nucl Med* 1996;37:1452-1456.
24. Norton JA, Sigel B, Baker RA, et al. Localization of an occult insulinoma by intraoperative ultrasonography. *Surgery* 1985;97:381-384.
25. Norton JA, Cromack DT, Shawher TH, et al. Intraoperative ultrasonographic localization of islet cell tumors. *Ann Surg* 1988;207:160-168.
26. Aprile C. Intraoperative radiolocalization of colorectal cancer: a review. *Int J Biol Markers* 1993;3:166-171.
27. Krenning EP, Kwekkeboom DJ, Pauwels S. Somatostatin receptor scintigraphy. In: Freeman LM, ed. *Nuclear medicine annual 1995*. New York: Raven Press; 1995:1-50.
28. Halpern SE, Haindel W, Beauregard J, et al. Scintigraphy with ¹¹¹In labeled monoclonal antitumor antibodies: kinetics, biodistribution and tumor detection. *Radiology* 1988;168:529-536.
29. Cohen AM, Martin EW, Lavery L, et al. Radioimmunoguided surgery using iodine 125 B72.3 in patients with colorectal cancer. *Arch Surg* 1991;126:349-352.
30. Curtet C, Vuillez JP, Daniel G, et al. Feasibility study of radioimmunoguided surgery of colorectal carcinomas using indium-111 CEA-specific monoclonal antibody. *Eur J Nucl Med* 1990;17:299-304.
31. Lamberts SWJ, Krenning EP, Reubi JC. The role of somatostatin and its analogs in the diagnosis and treatment of tumors. *Endocr Rev* 1991;12:450-482.
32. Ohta H, Yamamoto K, Endo K. A new imaging agent for medullary carcinoma of the thyroid. *J Nucl Med* 1984;25:323-325.
33. Sandler MP, Delbeke D. Radionuclides in endocrine imaging. *Radiol Clin North Am* 1993;31:909-921.
34. Reiners C. Imaging methods for medullary thyroid carcinoma. *Recent Results Cancer Res* 1992;125:125-145.
35. Baudin E, Lumbroso E, Schlumberger M, et al. Comparison of octreotide scintigraphy and conventional imaging in medullary thyroid carcinoma. *J Nucl Med* 1996;37:912-916.
36. Wahl RA, Röher HD. Surgery of C cell carcinoma of the thyroid. *Prog Surg* 1989;19:100-112.
37. Arnold MW, Hitchcock CL, Young DC, Burak WE Jr, Bertsch DJ, Martin EW Jr. Intra-abdominal patterns of disease dissemination in colorectal cancer identified using radioimmunoguided surgery. *Dis Colon Rectum* 1996;39:509-513.
38. Cote RJ, Houchens DP, Hitchcock CL, et al. Intraoperative detection of occult colon cancer micrometastases using ¹²⁵I-radiolabeled monoclonal antibody CC49. *Cancer* 1996;77:613-620.

Fluorine-18-Fluorodeoxyglucose and Carbon-11-Methionine Evaluation of Lymphadenopathy in Sarcoidosis

Yoshihito Yamada, Yoshitaka Uchida, Koichiro Tatsumi, Tetsuo Yamaguchi, Hiroshi Kimura, Hiroshi Kitahara and Takayuki Kuriyama

Departments of Chest Medicine and Radiology, School of Medicine, Chiba University, Chiba; and J.R. Tokyo Hospital, Tokyo, Japan

Uptake of ¹⁸F-fluorodeoxyglucose (FDG) and ¹¹C-methionine (Met) in mediastinum and hilar lymph nodes was studied using PET in 31 patients with sarcoidosis. The aim of our study was to examine whether these different tracers play a differential role in clinical assessment of pulmonary involvement. **Methods:** Fluorine-18-fluorodeoxyglucose and ¹¹C-Met PET were administered on different days. The differential absorption ratio of these tracers was calculated for the region of interest with the highest level of activity. Clinical reassessment of sarcoidosis was made at least 1 yr after the first PET examination. In seven patients whose lymph nodes still remained visible by other imagings at the time of reevaluation, the same PET study was performed again. **Results:** Both FDG and Met were accumulated in the lymph nodes in all but one patient. The FDG and Met uptake ratios in all patients were not correlated, but they could be divided into the FDG-dominant group (FDG/Met uptake ratio ≥ 2) and the Met-dominant group (FDG/Met uptake ratio < 2). Within each group, the FDG and Met uptake values were correlated. The rate of improvement assessed by clinical status and chest radiographs was considerably higher in the FDG- (78%) than

in the Met-dominant group (33%). In the seven patients of the repeated PET examination, their FDG/Met uptake ratios were generally unchanged after 1 yr. **Conclusion:** The results suggest that the FDG/Met uptake ratio using PET may reflect the differential granulomatous status in sarcoidosis and be a useful tool for pretreatment evaluation.

Key Words: PET; fluorine-18-fluorodeoxyglucose; carbon-11-methionine; sarcoidosis; mediastinum-bilateral lymphadenopathy

J Nucl Med 1998; 39:1160-1166

PET provides greater spatial resolution and quantitative analysis than other imaging techniques and may provide biophysiological and biochemical information superimposed on the anatomical topography. Fluorine-18-fluorodeoxyglucose (FDG) and L-methyl-¹¹C-methionine (Met) are widely applied tumor-seeking agents used together with PET, and they appear useful for assessing the biological behavior of malignant tumors (1-5). The mechanism of accumulating FDG into malignant tissue is due to its enhanced glucose metabolism. A high rate of glycolysis is a biochemical feature of malignant tissue. FDG is transported, phosphorylated and metabolically trapped intracellularly because it cannot be metabolized further and cannot

Received Mar. 11, 1997; revision accepted Oct. 13, 1997.

For correspondence or reprints contact: Koichiro Tatsumi, MD, Department of Chest Medicine, School of Medicine, Chiba University, 1-8-1 Inohana, Chuou-ku Chiba, Japan.

diffuse out of the cell. On the other hand, accumulation of Met into malignant tissue is thought to be due to increased amino acid metabolism such as enhanced amino acid active transport. Recent studies have suggested that FDG uptake may reflect the presence of inflammation such as the infiltration of macrophages, neutrophils and lymphocytes, and that Met uptake may be superior for estimating the presence of viable cancer cells (6–10). Because FDG and Met show different distributions in tumor tissue, these tracers may present different information in cancer imaging.

In patients with sarcoidosis, both FDG and Met may accumulate in the mediastinum and bilateral hilar lymph nodes because both tracers seem trapped in granulomatous inflammatory lesions, although the degree of their uptake may be different (6–10). The majority of patients with sarcoidosis have a favorable outcome, as granulomas disappear over time, probably due to a host-immune reaction. In some instances, however, lung fibrosis ensues with subsequent lung dysfunction possibly due to a granuloma-forming activity that overcomes the host-immune response. The different mechanisms for FDG and Met uptake may provide a differential role in the clinical management of sarcoidosis. Our study focused on the different uptake of FDG and Met in the mediastinum and bilateral hilar lymph nodes and whether the findings would provide a short-term prognosis for sarcoidosis patients.

MATERIALS AND METHODS

Patients

Thirty-one patients with pulmonary sarcoidosis (12 women, 19 men; age range 21–48 yr) were examined by PET using FDG and Met. The diagnosis was based on consistent clinical features along with transbronchial lung biopsy evidence of noncaseating epithelioid cell granulomas in all patients. Those who showed significant renal, cardiac, neurologic or ophthalmic organ involvement were excluded since these extrapulmonary disease manifestations require immediate therapy with corticosteroids. Chest radiographs were classified according to DeRemee (11). By chest-roentgenographic staging, 18 patients had Stage 1 (bilateral hilar lymphadenopathy without parenchymal infiltration) and 13 had Stage 2 (bilateral hilar lymphadenopathy with parenchymal infiltration) disease.

They were referred to our department between 1993 and 1995 because of abnormal shadows on chest radiographs or uveitis, and they presented with mediastinum-bilateral hilar lymphadenopathy (MBHL) greater than 10 mm in diameter on chest CT. Pulmonary involvement was assessed by chest radiographic imaging including CT findings. Extrathoracic involvement was considered present if ocular, skin, joint, peripheral lymph node, neurologic or other extrathoracic manifestations of sarcoidosis were documented. The serum angiotensin-converting enzyme (ACE) level was measured because it is one of most widely used markers of disease activity (12). None of these patients had undergone treatment for sarcoidosis before the PET run, nor did any receive treatment throughout the study. No patient had diabetes mellitus.

We assessed 24 patients as newly diagnosed, because their chest radiographs at about 1 yr before visiting our department had been normal. In the other 7 patients, similar abnormalities as at the time of diagnosis were detected in their chest radiographs about 1 yr previously.

PET Imaging

Synthesized by CYPRIS (cyclotron for production of radioisotope) and CUPID (clinical used positron-emitting isotope delivery) respectively, using a cyclotron system by Sumitomo Heavy Industries (Ehime, Japan), 148 MBq FDG and 555 MBq Met were

injected intravenously into each patient after they had been fasting for 24 hr. Because PET is influenced by nutritive conditions, it was performed after at least 6 hr of fasting and at the same time of day. Transmission scans were obtained for attenuation correction, and both FDG and Met were injected intravenously as a bolus after the transmission scans. Sixty minutes after FDG injection and 20 min after Met injection, sequential PET scans were performed only on the thorax for 20 min with a Headtome-III scanner (Shimadzu Corp., Tokyo, Japan) whose spatial resolution was 1.05 cm FWHM. Each patient was positioned to obtain PET images on a plane of the mediastinum and hilar lymph nodes as shown on the chest radiograph. In the tomographic mode providing a 51.2-cm square field of view, 12 slices, with a 8.2-mm thickness, of PET images were simultaneously obtained. Quantitative analysis was performed on a pixel-by-pixel (1 pixel = 16 mm²) basis. Tracer accumulation was measured in a 10- × 10-mm region of interest (ROI), and the ROI was set on the area where tracer activity was the highest. The location of the ROI for FDG and Met PET was different, because the sites of the highest tracer activity were not the same. Using the MBHL activity of tracers, the differential absorption ratio (DAR) of tracer to MBHL was calculated. We assumed that the specific gravity of MBHL and the body was 1, and the DAR was derived from the following equation:

$$\text{DAR} = \text{MBHL activity}/(\text{injected dose counts/body weight}).$$

A phantom test to correct the partial volume effect was not performed. In our preliminary study, we had examined the mediastinum and hilar regions in patients who did not suffer from sarcoidosis. Neither FDG nor Met was accumulated in those regions.

Gallium-67 Uptake in Mediastinum-Bilateral Hilar Lymphadenopathy

All patients had peripheral blood examination and whole-body ⁶⁷Ga scanning of the bronchoalveolar lavage (BAL) before PET imaging. Gallium-67 uptake in MBHL was graded as follows: (a) 0: no accumulation; (b) 1: distinct accumulation; and (c) 2: marked accumulation, as strong as in the liver. To minimize observer bias, the uptake grade was evaluated by nuclear medicine physicians without prior knowledge of the patient's clinical history, physical examination and laboratory data.

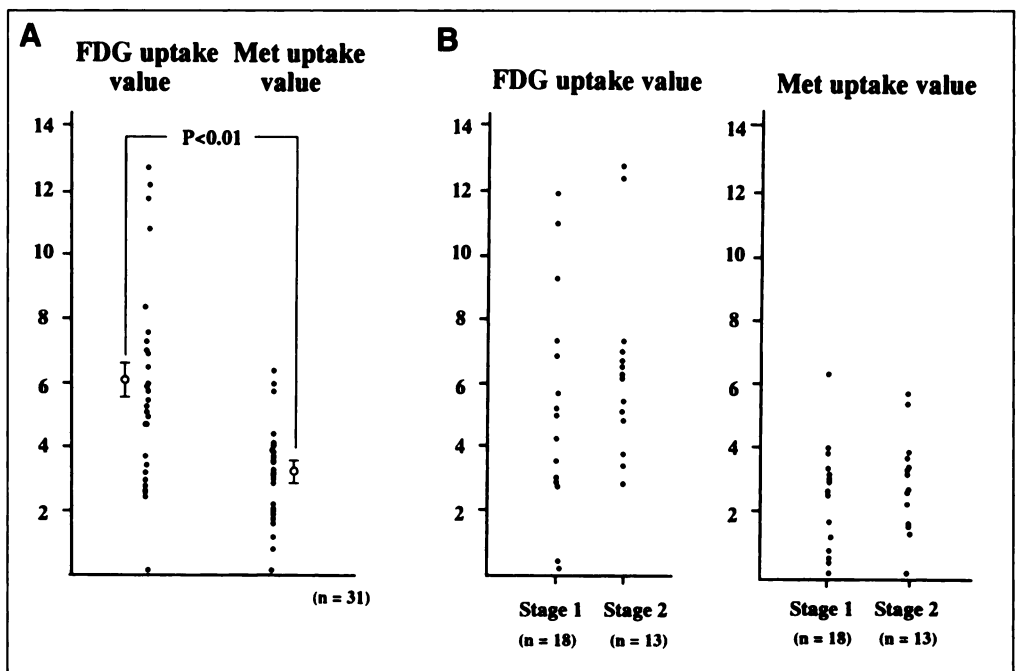
Bronchoalveolar Lavage

Bronchoalveolar cells were obtained by BAL in the standard manner (13) by instilling 150 ml sterile saline in 50-ml aliquots into a subsegment of the right middle lobe. BAL fluid (BALF) was then aspirated after each instillation. This procedure was performed at least 1 wk before the PET run. Cell numbers were counted and cell differentials were determined by counting over 500 cells on a cytocentrifuge smear stained with Wright-Giemsa. Small portions of cells were subjected to flow cytometric analysis for lymphocyte surface phenotyping (CD4 and CD8). The activities of soluble interleukin-2 receptor (sIL-2R), interleukin-1β (IL-1β), IL-1 receptor antagonist (IL-1ra), interferon-γ (IFN-γ) and tumor necrosis factor-α (TNF-α) in BALF were measured by ELISA methods.

Second PET Study and Clinical Reevaluation

We reevaluated the newly diagnosed 24 patients as to whether the disease had improved or deteriorated over the previous 12-mo period. Pulmonary and extrathoracic involvement were assessed similarly to the first PET examination. The serum ACE level was examined again and a decrease in its value was considered an index of improvement. Improvement also was defined as either disappearance or reduction of MBHL or parenchymal infiltration in the

FIGURE 1. (A) Distribution of FDG and Met uptake values to MBHL in patients with sarcoidosis. Mean FDG uptake value (6.02 ± 0.58) was significantly higher than Met (3.14 ± 0.29) ($p < 0.01$). Closed circles = individual patients; open circles with bar = mean \pm s.e. of each uptake value. (B) Distribution of FDG and Met uptake values to MBHL in Stage 1 and 2 sarcoidosis patients. There was no significant difference between Stages 1 and 2.



chest CT findings or extrathoracic involvement. The same PET runs were repeated in the 7 patients whose MBHL still existed at more than 10 mm in diameter at least 1 yr after the first PET examination to determine whether FDG or Met uptake had changed.

Statistical Analysis

The rates of accumulation of FDG and Met were compared by the Wilcoxon signed rank test. Correlations between serum ACE levels and BAL data were examined with the Pearson's correlation coefficient, and p values were determined by Fisher's A to Z. Correlation between PET and Ga was examined by Spearman's rank correlation test. The clinical features and short-term prognosis between the groups were compared by the chi-square test. The data between the first and second PET examinations were compared by the paired Student's t-test. Data are mean \pm s.e.

RESULTS

Met and FDG Uptake Values in Mediastinum-Bilateral Hilar Lymphadenopathy

Overall sensitivities of FDG and Met PET in detecting MBHL were both 97% (30/31 instances). The lesion in one

patient showed a negative result from PET diagnosis with both tracers, probably because the size of MBHL was the smallest (about 10 mm) among our patients. The mean FDG uptake value (6.02 ± 0.58) was significantly higher than that of Met (3.14 ± 0.29) ($p < 0.01$) (Fig. 1), although in some cases Met uptake was higher than that of FDG. No significant correlation was found between FDG and Met uptake values among all the patients (Fig. 2). There was no difference in either FDG or Met uptake when comparing patients in Stage 1 with those in Stage 2 (Fig. 1).

We divided the patients into two groups on the basis of the average FDG and Met uptake values of 6.02 and 3.14, respectively. One was the FDG-dominant group, whose FDG/Met uptake ratio was more than 2.0, and the other was the Met-dominant group, with a ratio of less than 2.0. In each group, there was significant linear correlation between FDG and Met uptake values (FDG-dominant group, $r = 0.93$, $p < 0.01$; Met-dominant group, $r = 0.41$, $p < 0.01$) (Fig. 2).

The incidence of pulmonary involvement in the first PET study was slightly higher in the FDG- (67%) than in the Met-dominant group (47%) ($p < 0.05$), while the incidence of

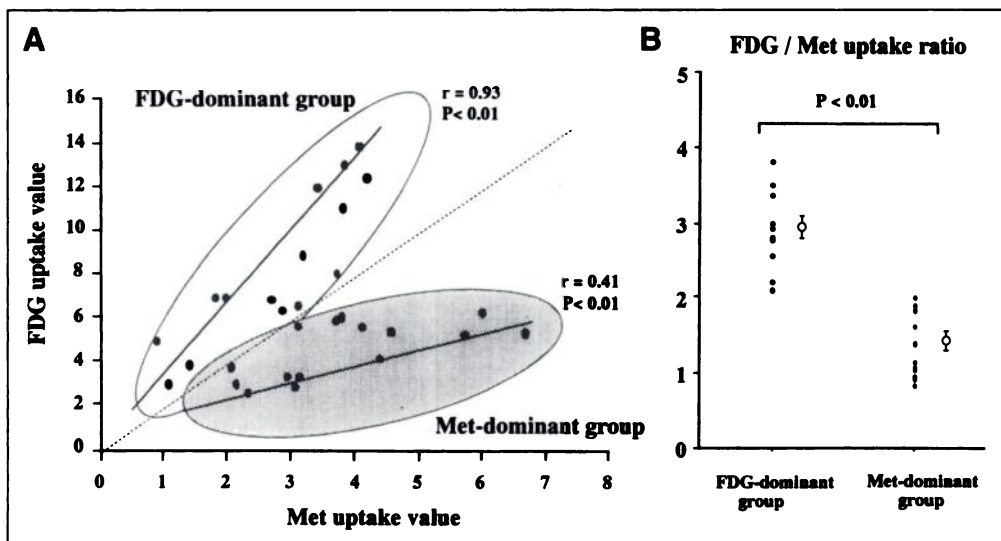


FIGURE 2. (A) Relationships between FDG and Met uptake values in all patients. Each closed circle represents a patient. Patients with FDG/Met uptake ratio of 2.0 or more were classified into FDG-dominant group and those under 2.0 into Met-dominant group. The dotted line represents $y = 2x$. FDG and Met uptake values were correlated within respective groups. (B) Distribution of FDG/Met uptake ratio in each group.

TABLE 1
Clinical Features at First PET Examination and Short-Term Prognosis in FDG- and Methionine-Dominant Groups

	First PET examination					
	Pulmonary involvement*		Extrathoracic involvement		Short-term prognosis (remission)*	
	(+)	(-)	(+)	(-)	(+)	(-)
FDG-dominant group (n = 9)	6/9 (67%)	3/9 (33%)	6/9 (67%)	3/9 (33%)	7/9 (78%)	2/9 (22%)
Methionine-dominant group (n = 15)	7/15 (47%)	8/15 (53%)	11/15 (73%)	4/15 (27%)	5/15 (33%)	10/15 (67%)

*Significant difference between FDG- and methionine-dominant groups ($p < 0.05$).

extrathoracic involvement was similar between the two groups (Table 1).

Comparison Between PET and Gallium-67 Scans

Gallium-67 uptake was correlated with FDG uptake ($r = 0.40$, $p < 0.05$) but not with Met uptake (Fig. 3). In patients whose ^{67}Ga uptake score was 2, the Met uptake value was high when the FDG uptake value was low, and the reverse was also true.

Correlation Between PET and Other Disease Indices

FDG uptake was correlated with the lymphocyte count ($r = 0.57$, $p < 0.01$) and sIL-2R ($r = 0.46$, $p < 0.05$) of BALF. Met uptake, on the other hand, was correlated with ACE ($r = 0.45$, $p < 0.05$), total cell ($r = 0.37$, $p < 0.05$) and lymphocyte counts ($r = 0.44$, $p < 0.05$), CD4/CD8 ($r = 0.47$, $p < 0.05$) and IL-1 β /IL-1ra ratios ($r = 0.65$, $p < 0.05$), and IL-1 β concentration ($r = 0.54$, $p = 0.12$) in BALF (Table 2).

Comparison Between FDG and Methionine-Dominant Groups

We compared the ACE levels, the cell counts, CD4/CD8 ratios and cytokines of BALF between the two groups. IL-1 β ($p < 0.05$) and IL-1 β /IL-1ra ($p < 0.01$) ratios in the Met-dominant group were significantly higher than those in the FDG-dominant group (Table 3).

Clinical Course

The disease activity in the seven patients who had the second PET runs decreased about 1 yr later judging from changes in their chest radiographs and ACE levels. Both FDG and Met uptake values also decreased ($p < 0.05$), although the ratio of the FDG/Met uptake value was unchanged (Table 4).

The short-term prognosis is shown in Table 1. No patients received any treatment after the initial PET scan. The FDG-dominant group showed a significantly greater remission incidence of MBHL compared to the Met-dominant group (78% versus 33%) ($p < 0.05$). The incidence of unchanged MBHL plus that of the appearance of pulmonary involvement, assessed by CT, was higher in the Met- (67%) than in the FDG-dominant group (22%). MBHL was unchanged in 40% (6 cases) of the Met-dominant group and in 11% (1 case) of the FDG-dominant group. The appearance rate of pulmonary involvement was 27% (4 cases) in the Met- and 11% (1 case) in the FDG-dominant group.

DISCUSSION

In our study, we examined whether PET could predict the clinical course of sarcoidosis by evaluating the different propensities of FDG and Met accumulation in MBHL. The FDG-dominant group had a higher rate of MBHL remission (78%) and a lower rate of appearance of pulmonary involvement plus unchanged MBHL (22%), while the Met-dominant group had a lower rate of MBHL remission (33%) and a higher rate of appearance of pulmonary involvement plus unchanged MBHL (67%). These results suggested that disease activity may not persist in the FDG-dominant group, while in the Met-dominant group the disease activity may continue to exist long-term and this group may develop chronic sarcoidosis of the lungs.

PET, used together with FDG, may be a useful imaging modality for evaluating disease activity in chronic inflammatory processes such as pulmonary sarcoidosis, although large

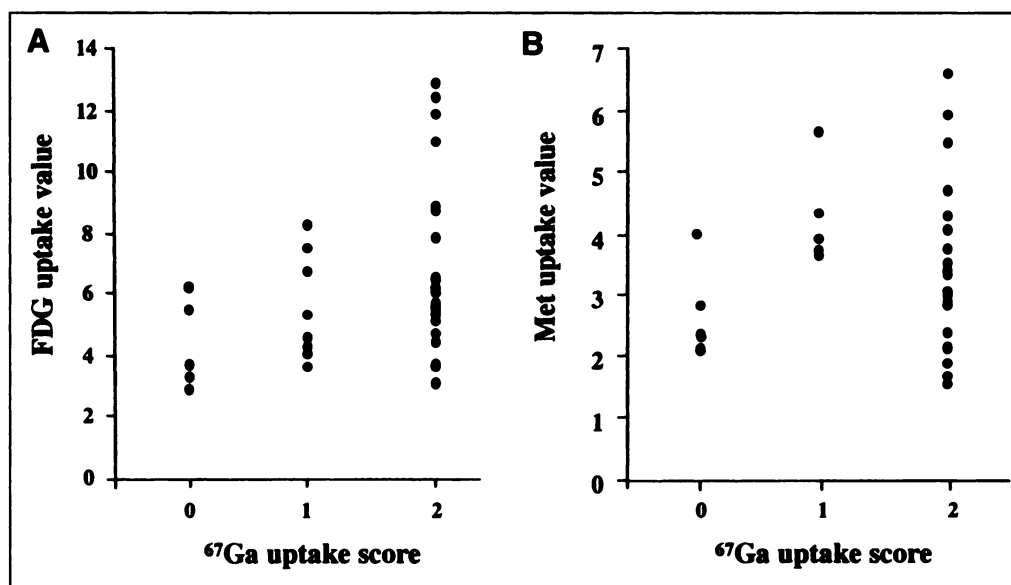


FIGURE 3. Relationship between (A) FDG and (B) Met uptake values and ^{67}Ga uptake score. Each closed circle represents a patient.

TABLE 2
Correlation Between FDG and Methionine Uptakes and Serum ACE and Cell Counts and Cytokines of BALF

Group	Serum					BALF					
	ACE (IU/L/37°C)	TCC (10 ⁵ /ml)	Lym (%)	Lym (10 ⁵ /ml)	CD4/CD8	sIL-2R (U/ml)	IL-1β (pg/ml)	IL-1ra (pg/ml)	IFN-γ (IU/ml)	TNF-α (pg/ml)	IL-1β/IL-1ra
FDG uptake	ns	ns	ns	r = 0.57*	ns	r = 0.46*	ns	ns	ns	ns	ns
Methionine uptake	r = 0.45*	r = 0.37*	ns	r = 0.44*	r = 0.47*	ns	r = 0.54*	ns	ns	ns	r = 0.65*

*p < 0.05.

ACE = angiotensin-converting enzyme; BALF = bronchoalveolar lavage fluid; TCC = total cell counts; Lym = lymphocyte; sIL-2R = soluble interleukin-2 receptor; IL-1β = interleukin-1β; IL-1ra = interleukin-1 receptor antagonist; IFN-γ = interferon-γ; TNF-α = tumor necrosis factor-α; ns = not significant.

scale, well-designed studies are warranted for defining PET's role in managing sarcoidosis patients (14-16). In our study, we assessed disease activity in the mediastinum and hilar lymph nodes using PET, as well as ⁶⁷Ga imaging, which has been established as a useful marker for evaluating sarcoidosis activity. Patients with a higher ⁶⁷Ga accumulation in the lymph nodes showed a higher uptake value of FDG. Lymph nodes about 10 mm in diameter seemed to be too small for accurate evaluation by FDG and Met uptake using PET. But, for those larger than 10 mm, both FDG and Met accumulated in the mediastinum and hilar lymph nodes suggesting sarcoid lymph nodes have a higher metabolic demand for both glucose and amino acids.

Sarcoidosis is a chronic systemic granulomatous disorder of unknown etiology and may involve the mediastinum and hilar lymph nodes. The characteristics of this disease are inflammatory reaction with activated lymphocyte and macrophage infiltration followed by formation of granulomas. While the majority of granulomas resolve without treatment, some progress to lung fibrosis. Patients diagnosed at an advanced age or those with many organs involved have been reported to have a poor prognosis (17), but the factors influencing the prognosis are yet unknown. There has been no generally accepted method for predicting the outcome of sarcoidosis, although histological examination at open-lung biopsy is a standard for disease activity and cellular infiltration. Serum ACE levels, ⁶⁷Ga scan and BAL cell counts also have been recognized as markers for pulmonary inflammation, but their relationship to the prognosis has not been established.

PET, using FDG and Met, has been reported clinically useful for malignant tumor diagnosis by evaluating hyper-metabolic demands for glucose and amino acids (1-5). FDG uptake may reflect tumor-host immune system response, because this tracer mainly accumulates in tumor-associated macrophages and young granulation tissues rather than in tumor cells (6,10). On the contrary, a microautoradiographic study (10) has demonstrated that Met uptake was achieved largely by viable cancer

cells, while the uptake by macrophages and granulation tissues was low. Mechanisms of FDG and Met uptake may provide a differentiating role for PET in evaluating physiological functions. In our present PET sarcoidosis study, the activities of granuloma formation and granuloma-associated immune cells may have been reflected by Met and FDG accumulations, respectively.

It is likely that FDG accumulates in MBHL because the sarcoidosis lesion is rich in inflammatory cells and granulomas. On the other hand, accumulation of Met in MBHL was considered to be low, because sarcoidosis is a granulomatous disorder and Met uptake in experimental inflammation has been reportedly low (10,18). The accumulation of Met in MBHL in sarcoidosis was clearly demonstrated in our study, although any correlation between histopathologic changes and uptake remains unclear.

FDG and Met uptake values showed no correlation among the total group of patients, because no patients were found whose FDG and Met uptake rates were equally high. In the patients with a high FDG uptake rate, the Met uptake was relatively low and vice versa. Our patients could be divided into two groups, FDG- and Met-dominant, based on the average values of FDG and Met uptake. FDG and Met uptake values were correlated within the respective groups. This phenomenon may be specific for sarcoidosis, because in malignant diseases a linear correlation was observed between FDG and Met uptake values (5) even though the pattern of the FDG PET image was reported to be nonspecific in sarcoidosis and malignant tumors, and it was difficult to differentiate between them (15). The second PET runs showed that the difference between the two groups may result not from the activity and condition but rather from a qualitative difference. The FDG/Met uptake ratio in the patients was unique in that it remained unchanged when no treatment was given during the clinical course. These results emphasize the heterogeneous nature of the inflammatory process in this disease.

Sarcoidosis may deteriorate or improve as a result of the

TABLE 3
Serum ACE and Cell Counts and Cytokines of BALF in FDG- and Methionine-Dominant Groups

Group	Serum					BALF					
	ACE (IU/L/37°C)	TCC (10 ⁵ /ml)	Lym (%)	Lym (10 ⁵ /ml)	CD4/CD8	sIL-2R (U/ml)	IL-1β (pg/ml)	IL-1ra (pg/ml)	IFN-γ (IU/ml)	TNF-α (pg/ml)	IL-1β/IL-1ra
FDG- dominant	19.6 ± 1.6	3.05 ± 0.64	39.6 ± 6.6	1.36 ± 0.29	5.14 ± 0.67	40.9 ± 11.4	650 ± 203	1485 ± 264	2.95 ± 0.22	2.76 ± 0.31	0.48 ± 0.16
Methionine- dominant	21.3 ± 1.3	2.76 ± 0.38	32.7 ± 5.4	1.01 ± 0.22	7.18 ± 1.21	29.4 ± 3.4	2000* ± 560	897 ± 91	3.78 ± 0.5	3.5 ± 0.67	1.79* ± 0.32

*p < 0.05.

ACE = angiotensin-converting enzyme; BALF = bronchoalveolar lavage fluid; TCC = total cell counts; Lym = lymphocyte; sIL-2R = soluble interleukin-2 receptor; IL-1β = interleukin-1β; IL-1ra = interleukin-1 receptor antagonist; IFN-γ = interferon-γ; TNF-α = tumor necrosis factor-α.

TABLE 4
Changes in ACE, FDG and Methionine Uptake Values Between First and Second PET Examinations

Patient no.	ACE (IU/L/37°C)		FDG uptake		Methionine uptake		FDG/Methionine uptake ratio	
	First examination	Second examination	First examination	Second examination	First examination	Second examination	First examination	Second examination
1	14.9	11.9	8.9	6.9	3.1	2.7	2.8	2.6
2	13.6	12.4	3.9	5.8	2.0	3.1	1.9	1.9
3	21.8	15.5	12.0	7.0	3.4	1.8	3.5	3.8
4	17.0	12.4	13.0	6.9	3.8	2.0	3.4	3.5
5	26.5	19.0	6.5	2.7	3.1	0.9	2.1	3.0
6	16.5	19.3	3.3	2.0	3.1	1.1	1.1	1.9
7	20.1	11.1	11.0	3.2	3.8	1.2	2.9	2.7
Mean	18.6	14.5*	8.4	4.9*	3.2	1.8*	2.5	2.8
±s.e.	1.7	1.3	1.5	0.8	0.2	0.3	0.3	0.3

*Significantly different from values at first PET study ($p < 0.05$).

balance of activities between forming granuloma and its resolution in the cytokine-network produced by activated lymphocytes, macrophages and epithelioid cells (19,20). In our study, we compared PET results with the production of cytokines in BALF. Met uptake was well correlated with IL-1 β and the IL-1 β /IL-1ra ratio and may reflect macrophage and/or epithelioid cell activation (19,21,22). On the other hand, FDG uptake was correlated with the activity of sIL-2R and may reflect lymphocyte activation (23,24). It is conceivable from previous studies that the pattern of uptake of FDG and Met manifests itself differently over a variety of proliferating cell fractions (6–10,25). It is likely that sarcoidosis patients with a high IL-1 β /IL-1ra ratio or high IL-1 β level have a poor prognosis and those with a high sIL-2R level have a good prognosis (24). The inflammatory and granulomatous reactions may persist with subsequent tissue dysfunction in patients with a higher Met uptake value, although the precise mechanisms remain unknown.

Although we observed our sarcoidosis patients only over the short term, they could be separated into two groups by the different prognosis at the first diagnosis by using PET with FDG and Met. The inflammatory and granulomatous activities seem to decrease over time without treatment giving a good prognosis to the FDG-dominant group. On the other hand, the disease activity is likely to continue, resulting in pulmonary involvement, and giving a poor prognosis for the Met-dominant group. These results suggest that FDG and Met uptake in MBHL, as measured by PET, may reveal the activities of the host-immune response and granuloma formation, respectively. Further studies of the mechanisms of FDG and Met uptake into lymph nodes and long-term follow-up of disease activity with PET would be useful.

CONCLUSION

Sarcoid lymph nodes, less than 10 mm in diameter, seem difficult to accurately evaluate by PET due to resolution difficulties. Although glucose and amino acid metabolism may increase in most sarcoidosis patients, the wide variation in FDG and Met uptake may imply heterogeneity of lymph node metabolism. Both FDG and Met uptakes were indices of disease activity, but they may provide different information. A good prognosis may be expected for the FDG-dominant group, but not for the Met-dominant group. PET is one of the most reliable, yet noninvasive, imaging techniques for qualitatively evaluating disease activity, although the PET procedure may have limitations related to metabolism.

ACKNOWLEDGMENTS

We thank Dr. Sonoko Nagai (Second Department of Medicine, Chest Disease Institute, Kyoto University) for her supportive advice.

REFERENCES

- Fujiwara T, Matsuzawa T, Kubota K, et al. Relationship between histologic type of primary lung cancer and carbon-11-L-methionine uptake with positron emission tomography. *J Nucl Med* 1989;30:33–37.
- Kubota K, Matsuzawa T, Fujiwara T, et al. Differential diagnosis of lung tumor with PET: a prospective study. *J Nucl Med* 1990;31:1927–1932.
- Leskinen-Kallio S, Nagren K, Lehtikoinen P, Ruotsalainen U, Teras M, Joensuu H. Carbon-11-methionine and PET as an effective method to image head and neck cancer. *J Nucl Med* 1992;33:691–695.
- Okada J, Yoshikawa K, Itami M, et al. PET using fluorine-18-fluorodeoxyglucose in malignant lymphoma: a comparison with proliferative activity. *J Nucl Med* 1992;33:325–329.
- Inoue T, Kim EE, Wong FCL, et al. Comparison of fluorine-18-fluorodeoxyglucose and carbon-11-methionine PET in detection of malignant tumors. *J Nucl Med* 1996;37:1472–1476.
- Kubota R, Yamada S, Kubota K, Ishiwata K, Tamahashi N, Ido T. Intratumoral distribution of fluorine-18-fluorodeoxyglucose in vivo: high accumulation in macrophages and granulation tissues studied by microautoradiography. *J Nucl Med* 1992;33:1972–1980.
- Miyazawa H, Arai T, Iio M, Hara T. PET imaging of non-small-cell lung carcinoma with carbon-11-methionine: relationship between radioactivity uptake and flow-cytometric parameters. *J Nucl Med* 1993;34:1886–1891.
- Kubota R, Kubota K, Yamada S, Tada M, Ido T, Tamahashi N. Microautoradiographic study for the differentiation of intratumoral macrophages, granulation tissues and cancer cells by the dynamics of fluorine-18-fluorodeoxyglucose uptake. *J Nucl Med* 1994;35:104–112.
- Minn H, Clavo AC, Grenman R, Wahl RL. In vitro comparison of cell proliferation kinetics and uptake of tritiated fluorodeoxyglucose and L-methionine in squamous-cell carcinoma of the head and neck. *J Nucl Med* 1995;36:252–258.
- Kubota R, Kubota K, Yamada S, et al. Methionine uptake by tumor tissue: a microautoradiographic comparison with FDG. *J Nucl Med* 1995;36:484–492.
- DeRemee RA. The chest roentgenology of sarcoidosis. In: Lieberman J, ed. *Sarcoidosis*. Orlando: Grune and Stratton; 1985:117–135.
- Meeting Report. Consensus conference: activity of sarcoidosis. *Eur Respir J* 1994;7:624–627.
- Reynolds HY. Bronchoalveolar lavage. *Am Rev Respir Dis* 1987;135:250–263.
- Alavi A, Buchpiguel CA, Loessner A. Is there a role for FDG-PET imaging in the management of patients with sarcoidosis? *J Nucl Med* 1994;35:1650–1652.
- Lewis PJ, Salama A. Uptake of fluorine-18-fluorodeoxyglucose in sarcoidosis. *J Nucl Med* 1994;35:1647–1649.
- Brudin LH, Valind SO, Rhodes CG, et al. Fluorine-18 deoxyglucose uptake in sarcoidosis measured with positron emission tomography. *Eur J Nucl Med* 1994;21:297–305.
- Israel HL, Karlin P, Menduke H, DeLisser OG. Factors affecting outcome of sarcoidosis. Influence of race, extrathoracic involvement, and initial radiologic lung lesions. *Ann NY Acad Sci* 1986;465:609–618.
- Kubota K, Matsuzawa T, Fujiwara T, et al. Differential diagnosis of AH109A tumor and inflammation by radiosintigraphy with L-[methyl-¹¹C] methionine. *Jpn J Cancer Res* 1989;80:778–782.
- Daniele RP, Rossman MD, Kern JA, Elias JA. Pathogenesis of sarcoidosis. *State of the Art Chest* 1986;89:174S–177S.
- Kelley J. Cytokines of the lung. *Am Rev Respir Dis* 1990;141:765–788.
- Nagai S, Aung H, Takeuchi M, Kusume K, Izumi T. IL-1 and IL-1 inhibitory activity in the culture supernatants of alveolar macrophages from patients with interstitial lung diseases. *Chest* 1991;99:674–680.
- Takeuchi M, Nagai S, Nakada H, Aung H, Satake N, Kaneshima H, Izumi T.

- Characterization of IL-1 inhibitory factor released from human alveolar macrophages as IL-1 receptor antagonist. *Clin Exp Immunol* 1992;88:181-187.
23. Muller-Quemheim J, Pfeifer S, Mannel D, Strausz J, Ferlinz R. Lung-restricted activation of the alveolar macrophage/monocyte system in pulmonary sarcoidosis. *Am Rev Respir Dis* 1992;145:187-192.
24. Yamaguchi E, Okazaki N, Tsuneta Y, Abe S, Terai T, Kawakami Y. Interleukins in pulmonary sarcoidosis. Dissociative correlations of lung interleukins 1 and 2 with the intensity of alveolitis. *Am Rev Respir Dis* 1988;138:645-651.
25. Abdel-Dayem HM, Scott A, Macapinlac H, Larson S. Tracer imaging in lung cancer. *Eur J Nucl Med* 1994;21:57-81.

Technetium-99m-MIBI in Primary and Recurrent Head and Neck Tumors: Contribution of Bone SPECT Image Fusion

Thomas Leitha, Christoph Glaser, Martha Pruckmayer, Michael Rasse, Werner Millesi, Susanna Lang, Christian Nasel, Werner Backfrieder and Franz Kainberger

University Clinics of Nuclear Medicine, Maxillofacial Surgery, Radiology and Pathology, Department of Biomedical Engineering and Physics, Vienna, Austria

We prospectively investigated 200 patients with the clinical suspicion for head and neck tumors. The final diagnoses were 94 primary and 56 (37 confirmed, 19 excluded) recurrent squamous cell carcinomas (SCCs), 3 primary and 7 (4 confirmed, 3 excluded) recurrent adenoid cystic carcinomas (ACCs), 6 non-Hodgkin's lymphomas, 10 distant metastases, 6 other malignancies, 10 inflammatory and 8 other nonmalignant conditions. **Methods:** Bone (600 MBq ^{99m}Tc -3,3-diphosphono-1,2-propane dicarboxylic acid tetrasodium salt) and hexakis-2-methoxyisobutyl isonitrile (MIBI) (600 MBq ^{99m}Tc -MIBI) SPECT were both performed under identical conditions (triple-head gamma camera; ultra-high-resolution, parallel-hole collimators; three-dimensional postfiltering) and judged independently and after superimposition. The results were compared to the results of biopsy, surgery and CT. **Results:** The overall sensitivity/specificity of MIBI was 90%/78% for tumor detection and 90%/95% for the identification of malignant lymph node involvement (CT: 79%/66%, respectively 90%/79%). In the subgroup of recurrent SCC and ACC the sensitivity/specificity for tumor detection was 95%/71% for MIBI versus 78%/68% for CT. The isolated assessment of bone SPECT had a sensitivity/specificity of 100%/17% for osseous tumor spread. Image fusion of MIBI and bone SPECT differentiated between regio-local bone involvement and inflammatory changes and increased the specificity of bone SPECT to 100% in primary staging. Tumor size, stage, histology and pretreatment had no statistically significant effect on tracer uptake or diagnostic utility of scintigraphy. **Conclusion:** We propose the combined ^{99m}Tc -MIBI and bone ultra-high resolution SPECT as a highly useful imaging approach in the primary and secondary staging in patients with suspected malignancies in the head and neck region. The high specificity for malignancies in the head and neck region may be used in the differential diagnosis between head and neck malignancies and inflammatory disease in patients with the accidental finding of enlarged lymph nodes and no clinical signs of a primary tumor. Image fusion with bone scanning is mandatory for the topographical orientation and increases the specificity of bone scanning to differentiate between inflammatory or malignant causes of increased bone metabolism.

Key Words: technetium-99m-hexakis-2-methoxyisobutyl isonitrile; image fusion; head and neck cancer; bone scan; staging

J Nucl Med 1998; 39:1166-1171

Cancer of the head and neck accounts for 4%-5% of all cancers in the western world (1), with much higher incidences in other areas. Ninety-five percent of the cancers arise from squamous epithelium (SSC) and about 1.5% of head and neck cancers are adenoid cystic carcinomas (ACCs) that arise mainly from the minor salivary glands. Lymphomas account for 1.5% of cases of head and neck cancer. The remaining 2% of cancers of the head and neck are melanomas, soft-tissue tumors and thyroid and parathyroid tumors.

Limited cancer stages, especially in the oral cavity, are accurately assessed by clinical evaluation but tumor depth is clinically underestimated in more advanced stages (2). Additionally, in a prospective evaluation of 81 consecutive patients, 17% of multiple primary lesions were clinically overlooked (3). The use of the appropriate imaging technology depends on the availability, expertise and experience of the radiologist and on the quality of the equipment available (4). The advantages of CT include (a) better sensitivity to bone destruction; (b) better delineation of nodal architecture; (c) lower costs; (d) higher availability; and (e) lower rate of claustrophobia. The advantages of MRI include (a) no necessity for iodinated contrast media; (b) less dental artifacts; (c) multiplanar acquisition; (d) detailed imaging of soft-tissue invasion outside the nasopharynx; and (e) retropharyngeal node involvement (5). Nevertheless, MRI is hampered in the detection of bone erosion (6), which is crucial for planning the extent of surgery. CT remains the gold standard in staging of head and neck tumors in many institutions (7), including ours.

Despite advances in surgical technique and adjuvant radiochemotherapy, recurrent disease ultimately develops in about half of patients with squamous cell carcinoma (SCC) and ACC. Morphological imaging techniques are of limited use in the secondary staging of patients with severe anatomical changes after radiotherapy, surgery and flap reconstruction in the mouth floor.

In clinical routine, many patients present with the accidental finding of enlarged lymph nodes in the head and neck region. In the absence of visible pathologies of the mucosa, the differential diagnosis has to be made between an occult but advanced primary tumor (most likely in the diagnostic cold spot of the nasopharynx), systemic malignancies or inflammatory lymph node enlargement.

At present, nuclear medicine plays only a limited role in the

Received Apr. 23, 1997; revision accepted Oct. 13, 1997.
For correspondence or reprints contact: Thomas Leitha, MD, University Clinic Nuclear Medicine, Waehringerguertel 18-20, A-1090 Vienna, Austria.